

**Rochester Institute of Technology**

Department of Mechanical and Manufacturing Engineering Technology

*Manufacturing and Mechanical Systems Integration*



# **ABB CRB 15000 Machine Vision Robotic Tool Grinder**

By: Isaac R. Vasquez

May 2024

# Acknowledgements

This research was conducted and completed with the support of the following individuals:

- Dr. Marten Anselm
- Dr. Robert Garrick
- Professor Reynaldo Kelly
- Professor Michael Caldwell
- Trevor McGregor (Calvary Robotics)
- Adam Blumrath and Jarrod Pomerantz (RIT Students)

# Contents

<b>1</b>	<b>Abstract</b>	<b>4</b>
<b>2</b>	<b>Introduction</b>	<b>5</b>
2.1	Background . . . . .	6
2.2	Purpose Statement . . . . .	6
2.3	Significance of Study . . . . .	6
<b>3</b>	<b>Literature Review</b>	<b>7</b>
3.1	Focus on Robotic Deburring Application . . . . .	7
3.1.1	Focus On Vision Tools . . . . .	8
<b>4</b>	<b>Methodology</b>	<b>10</b>
4.1	Research Questions . . . . .	10
4.2	System Overview . . . . .	10
<b>5</b>	<b>Design Phases</b>	<b>12</b>
5.1	Mechanical Design . . . . .	12
5.1.1	Work cell Work Envelope . . . . .	12
5.1.2	Tooling Fixtures . . . . .	13
5.1.3	Work Cell Layout . . . . .	15
5.2	Electrical Design . . . . .	16
5.2.1	Load and Fuse Calculations . . . . .	16
5.2.2	Wiring Color . . . . .	16
5.2.3	Component Selection . . . . .	16
5.3	Vision Design . . . . .	17
5.3.1	Vision Environment . . . . .	17
5.3.2	Camera . . . . .	18
5.3.3	Lens . . . . .	18
5.3.4	Backlight . . . . .	19
5.4	Design Decisions . . . . .	19
5.4.1	Force Control . . . . .	19
5.4.2	Belt Sander . . . . .	20
<b>6</b>	<b>Build Phases</b>	<b>21</b>
6.1	Mechanical Build Phase . . . . .	21
6.1.1	Additive Manufacturing . . . . .	21
6.1.2	Fabrication . . . . .	21
6.2	Electrical Build . . . . .	24
6.2.1	PLC Panel Wiring and Layout . . . . .	24
6.2.2	External Device Wiring . . . . .	25
6.3	Fully Assembled Cell . . . . .	27
<b>7</b>	<b>Software Deployment</b>	<b>28</b>
7.1	Network Design . . . . .	28
7.2	PLC . . . . .	28
7.2.1	Generating Device Modules . . . . .	28

7.2.2	Create Local Tags . . . . .	30
7.3	Robotic Integration . . . . .	31
7.3.1	Robotic Controller Configuration . . . . .	31
7.3.2	Data Types . . . . .	33
7.3.3	I/O Configuration . . . . .	34
7.3.4	RAPID Procedures . . . . .	35
7.4	Vision Integration . . . . .	36
7.4.1	Connecting to Camera . . . . .	36
7.4.2	Image Processing . . . . .	37
7.4.3	Data Transfer to PLC . . . . .	39
<b>8</b>	<b>Data and Results</b>	<b>40</b>
8.1	Mechanical Verification . . . . .	40
8.2	Statistical Verification . . . . .	40
<b>9</b>	<b>Discussion</b>	<b>42</b>
9.1	Grind Performance . . . . .	42
<b>10</b>	<b>Conclusion</b>	<b>43</b>
10.1	Future Improvements . . . . .	43
10.2	Project Hurdles and Lessons Learned . . . . .	43
<b>11</b>	<b>Appendix A</b>	<b>46</b>
<b>12</b>	<b>Appendix B</b>	<b>48</b>



# 1 Abstract

In contemporary engineering, there is a growing emphasis on automating manufacturing processes, particularly those historically deemed repetitive and mundane for humans. This shift stems from the recognition of inherent risks posed by manual tasks, often prone to errors and inconsistencies. As such, engineers increasingly turn to robotic systems and machine vision technologies to develop precise, reliable, and automated alternatives. This capstone report presents a comprehensive examination aimed at validating the efficacy of automating a manual tool grinding process. Specifically, it focuses on reducing risks associated with the current manual process, which involves applying a 45° chamfer to a rectangular tool. Through systematic analysis and experimentation, this study demonstrates the potential of automated solutions in mitigating risks and enhancing efficiency within manufacturing operations. The findings reveal that the implementation of automated systems successfully reduced errors and increased repeatability within .200 degrees from nominal, thus validating the feasibility and effectiveness of automation in enhancing manufacturing processes.

The work cell is built in the RIT Automation Lab SLA-2450 and integrates the following components:

- ABB CRB 15000 GoFa Collaborative robot with Omnicore 30 Controller
  - ABB RobotStudio
- Belt Sander
- Allen Bradley 5370 1769 L16ER-BB1B CompactLogix Programmable Logic Controller (PLC)
  - Studio5000 Logix Designer
- Cognex In-Sight 5100 (640x480px)
  - In-Sight Explorer
- Fujinon HF35HA-1S 35mm (lens)
- Moritex CV-FL-63x60B-M12 (backlight)

*Keywords:* Machine Vision, Robotics, Tool Grinding, Automation

## 2 Introduction

The Robotics and Automation Lab in Slaughter Hall 2450 at the Rochester Institute of Technology provides students with opportunities to learn and develop their PLC programming and automation control theory skills. Located in the lab is a mobile work cell where a ABB CRB 15000 GoFa Collaborative robot is mounted on a cart with a work place made of aluminum extrusion. The robot was purchased with the intent of allowing graduate students to complete their robotics research and capstones on a robot that was not utilized by the undergraduate robotics courses. With that being, the cell and the integration of this robotic application provides an excellent opportunity for the robotics professors in our department to demonstrate to their classes an industrial application of robotics. The purchasing of this robotic cell was made possible by the generous donation from Calvary Robotics.

Throughout the report there are a variety of terms used. Below are some descriptions of terms with and visuals of the equipment used in the system.

- Allen Bradley 5370 1769 L16ER-BB1B CompactLogix Programmable Logic Controller (PLC)
  - A PLC is a rugged computer that is standard in industrial automation projects. PLCs continuously monitor the states of device inputs to make decisions based on a custom program written to control the state of output devices. The CompactLogix PLC is Allen Bradley's compact PLC line.



- ABB Omnicore C30 Robot Controller
  - A robot controller is needed for all robots and serves as the central processing unit executing the robot program, I/Os, and coordinating the motion of the robotic joints. The Omnicore C30 robot is ABB's compact controller line.



## **2.1 Background**

In traditional tool grinding applications, reliance on manual labor and human skill dependency introduces variability and the potential for errors, impacting the repeatability and precision. Moreover, the pursuit of high precision often comes at the cost of slower production rates. Beyond chamfering edges, deburring tasks are also commonly performed manually, further illustrating the need for automation in manufacturing processes. By implementing an automated solution, the aim is to enhance consistency, accuracy, and efficiency in tool manufacturing, ultimately reducing errors and improving overall productivity. This project not only addresses the specific challenges of chamfering but also highlights the broader potential for automation to revolutionize various manual tasks in the manufacturing industry

## **2.2 Purpose Statement**

The purpose of this project is to develop an automated tool grinding work cell that provides a repeatable 45 degree chamfer grind on a singular edge of a rectangular tool. The grind will be conducted by efforts of a robotic arm taking the tool to a belt sander in which will perform the grind undergo validation by means of machine vision integration.

## **2.3 Significance of Study**

The results of this project are also intended to allow for future leveraging by graduate students seeking robotic setups that integrate machine vision, automation, and pressure applications. Furthermore, the desired work cell is intended to be modular such that future work can be added removed after the conclusion of this research.

## 3 Literature Review

### 3.1 Focus on Robotic Deburring Application

Graduate researchers at McMaster University investigated the implementation of an active end effector-based force control system for robotic deburring using a PUMA-560 robot. The primary objective is to achieve precise chamfer depth with minimal surface roughness by minimizing the variance in the normal chamfering force in real-time. The study evaluates several force control algorithms designed to achieve this goal. Key points of the research:

1. Robotic deburring is explored as an alternative to manual deburring, driven by the high cost of manual deburring, which can account for a substantial portion of the total cost.
2. The control of the chamfer depth is of utmost importance, and this research focuses on controlling it with non-compliant cutting tools.
3. To maintain a consistent chamfer depth, it is essential to control the normal force during deburring.
4. While a robot arm can provide coarse motion around the part, a specialized end effector is used for fine motion control, especially in sharp corners.
5. The research incorporates active end effectors with impedance control to achieve precise chamfering and material removal rate control.
6. The control objective is to minimize the chamfer surface roughness by minimizing the variance in the normal force during deburring.
7. The research project emphasizes the development of a fine motion control system for the end effector, assuming that the robot trajectory is known a priori.

This research provided insight into potential solutions within robotic tool deburring using force control (see Figure 1). While the elected method of force control conducted in the development of this capstone's research was an ABB Force Control license, the methods and areas of research such as understanding the importance behind fine motion control systems for the end effector provided insight into how to better improve the workcell. In addition, it highlighted the importance of being able to control the Normal Force applied to the contacted forces. That was leveraged in this research as the force was strictly applied in one Cartesian direction.

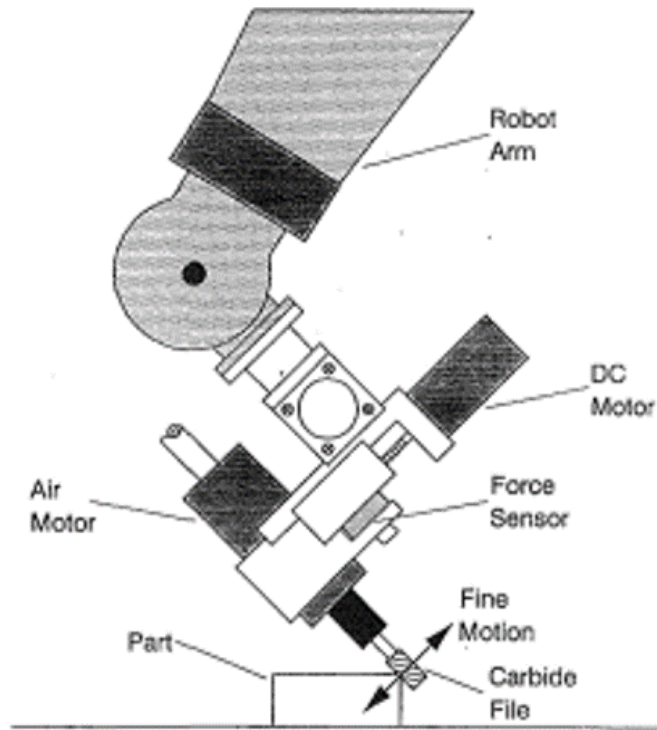


**Fig. 8 Experimental setup for the real-time control tests**

Figure 1: Example of a Robotic Deburring Solution [3]

### 3.1.1 Focus On Vision Tools

Researchers by the names of Anup Pillai, Shital Chiddarwar, M. R. Rahul, and Mohsin Dalvi developed a paper highlighting ideal configurations for image acquisition setup (see Figure 2). The paper illustrates a configuration for image acquisition that promote minimum noise and interference with lights for deburring applications. The concept of a box enclosing setup was debated given the potential for FOD (grind debris) to get on the lens. However, further design considerations of the cell layout and newly provided space constraints altered this selection.

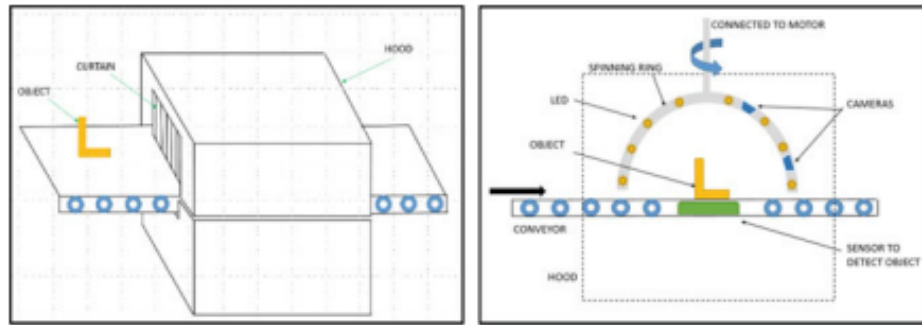


**Fig. 2** Basic design of image acquisition setup



**Fig. 3** Image acquisition setup

Figure 2: Example of a Image Acquisition [6]

This literature review was not limited to merely these two papers; rather, it encompassed a comprehensive examination of existing research and scholarly works in the field. By synthesizing insights from a diverse range of sources, including academic journals, conference proceedings, books, and standard engineering-based websites, a holistic understanding of machine vision and robotic deburring was attained. The synthesis of findings from multiple studies provided valuable context, highlighted key trends, and laid the groundwork for understanding the completed research in this field. With that being said a direct application utilizing a CRB15000 GoFa was not identified.

## 4 Methodology

### 4.1 Research Questions

The research questions that will be addressed in this report include:

- How does the integration of robotic arm technology and machine vision systems enhance the repeatability and accuracy of chamfer grinding processes in comparison to manual labor?
- What are the key design considerations for developing a safe yet modular tool grinding work cell that allows for seamless integration of additional functionalities beyond chamfer grinding?

### 4.2 System Overview

Before designing the work cell, it was crucial to identify the system flow chart and clearly define all interactions and dependencies between components. This ensured a systematic approach to the design process and facilitated efficient communication. The system flow chart served as a visual roadmap, illustrating the sequence of operations and data flow within the work cell. Additionally, the system flow chart provided a valuable reference for troubleshooting and maintenance activities throughout the project lifecycle (see Figure 3).

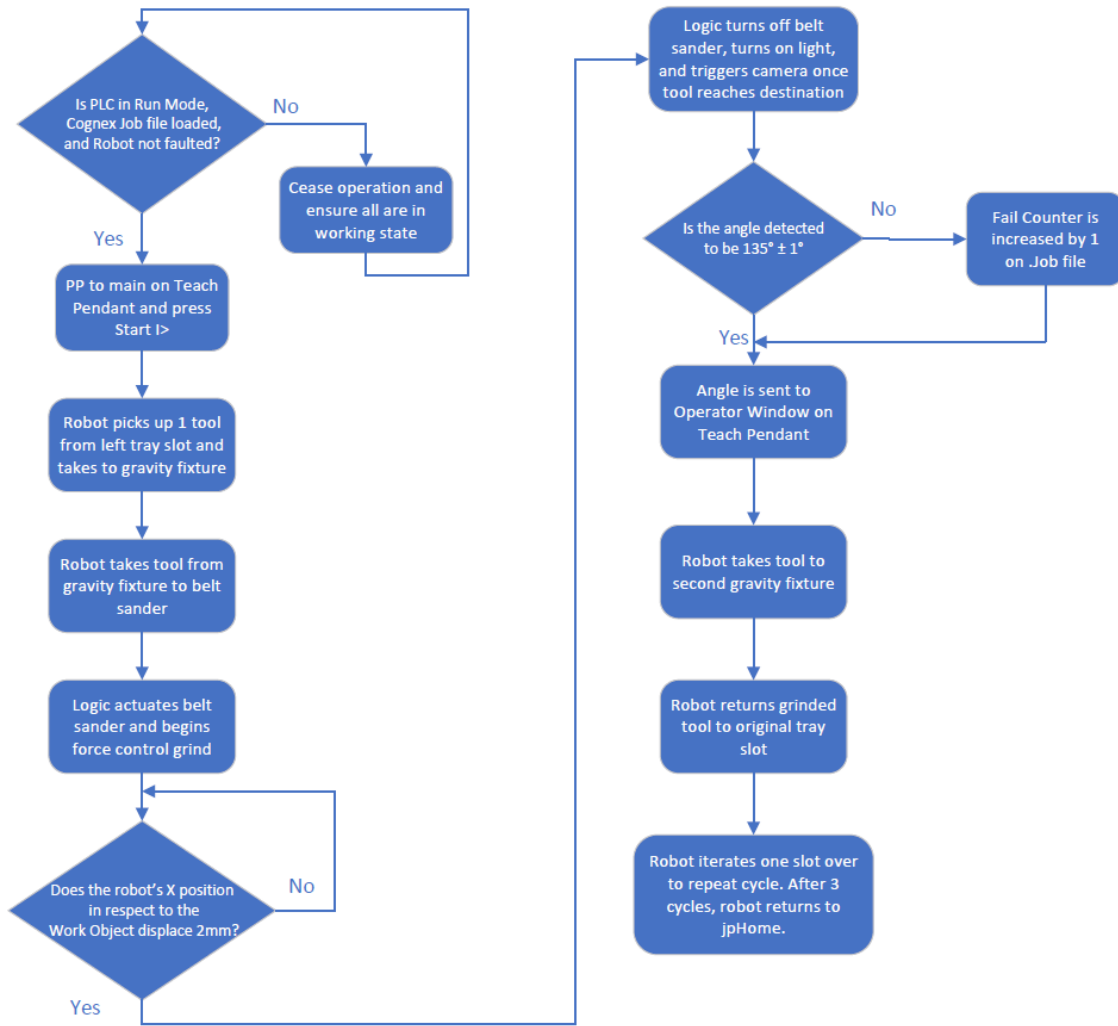


Figure 3: System Flowchart of Work cell



## 5 Design Phases

### 5.1 Mechanical Design

#### 5.1.1 Work cell Work Envelope

The first phase in the design process of the work cell was the mechanical design phase. This stage encompassed crucial tasks such as conceptualizing the work cell layout, crafting fixtures, and integrating safety measures and advanced technologies. Before proceeding with the layout planning, it was imperative to account for the specific limitations of the work cell. For instance, the dimensions of the work cell were inherently dictated by the dimensions of the cart. The cart, featuring a work envelope measuring 590.01mm in length and 621.20mm in width, was defined by the T-slotted table top upon which the robot was securely mounted (refer to Figure 4). While this constraint was intrinsic to the robotic cart provided by Empire Automation Systems, it also ensured the work cell's modularity and mobility. Notably, the cart's dimensions allowed it to effortlessly navigate through standard door frames. Furthermore, it is worth mentioning that the work envelope of the cart comfortably fell within the operational range of the robot utilized in this system. The robot, a 6-axis CRB 15000 model, boasted a 0.95m reach and a substantial 5kg payload capacity. (see Figure 5).

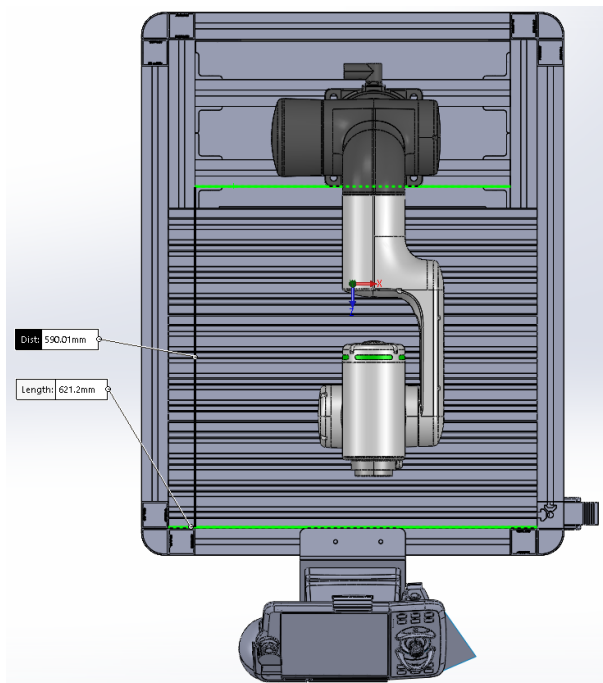


Figure 4: Dimensions of Cart Workspace

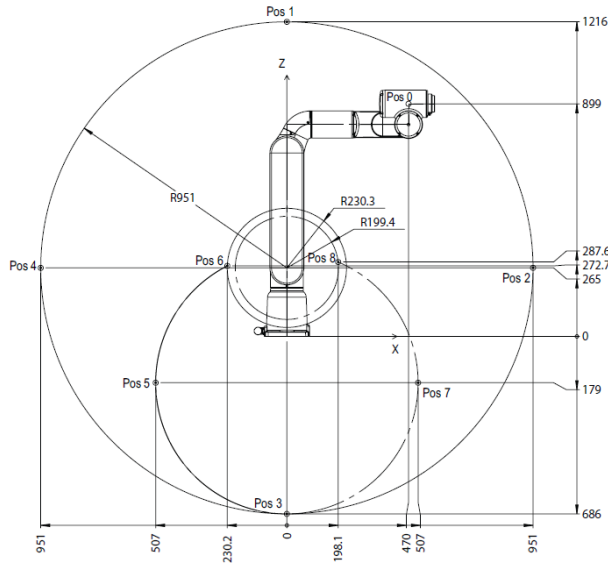


Figure 5: CRB 15000 Working Range

### 5.1.2 Tooling Fixtures

Once the system flowchart was established and the work cell constraints were identified, it was time to begin laying out the fixtures that would be required. The orientation in which the tool would be ground was crucial for determining how the robot must pick up the tool. This is where the concept of a gravity fixture emerged. In robotic machine-tending applications, parts often arrive on a tray in an unordered fashion, making it challenging to pick up the tool consistently. This issue had to be addressed, as the position of the tools could not be controlled in the tray (see Figure 6a). After pickup from the tray, the robot will place the tool in a fixture that utilizes gravity to configure it in the same position each time, allowing for repeatable tool pickup (see Figure 6b).

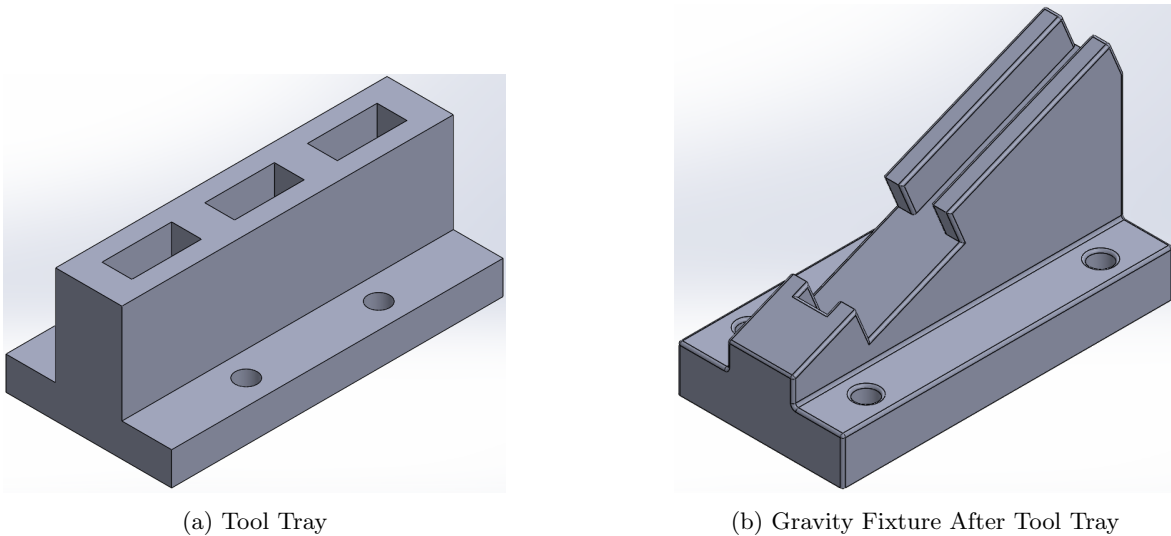


Figure 6: Tool Tray and Gravity Fixture

Given that the tool was to be gripped by the robot's EOAT in a horizontal manner, it had to be replaced in the vertical standing tool tray. To achieve this reorientation of the tool to a vertical position,

another intermediate gravity tray was used. This tray allowed for the tool to be placed and then re-picked up by the gripper's jaws descending along the sides, securing it in a vertical orientation. Once picked up in the vertical orientation, the tool is placed back into its original position in the tool tray for the process to repeat again for the remaining tools (see Figure 7).

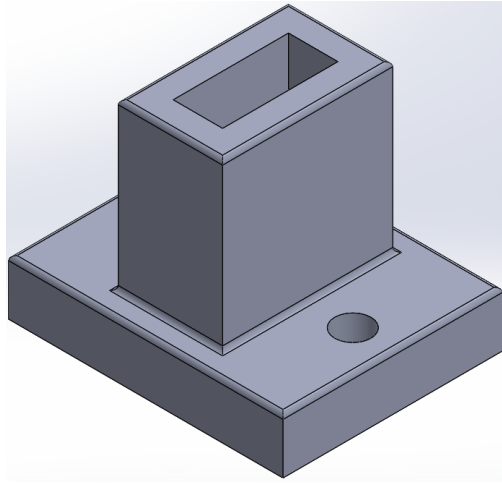
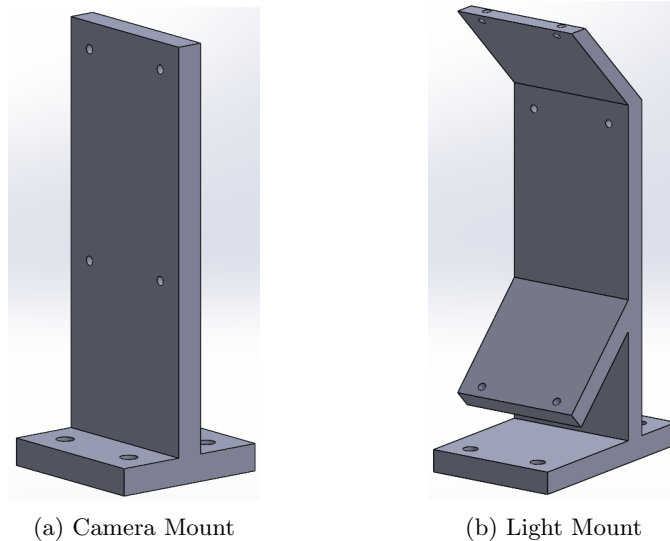


Figure 7: Vertical Gravity Fixture

To ensure consistent and repeatable image capture, mounts were specifically designed for both the camera and backlight. Positioned at the front of the cart, these mounts enable the robot to position the tool optimally between them, resulting in the best possible images for machine vision processing (see Figure 8a and 8b).



(a) Camera Mount

(b) Light Mount

Figure 8: Camera and Light Mounts

The last component to be designed was a protective casing for the belt sander. Due to the nature of belt sanders, they tend to scatter chips of ground material in their vicinity during operation. To mitigate this issue and prevent debris from interfering with the camera lens and backlight, as well as to provide a measure of safety for personnel operating the cell nearby, a casing was devised to enclose the belt sander. The casing

was designed with an open top and slit in the back to allow for a small vacuum hose to fit through and clean the area of excess debris and chips (see Figure 9).

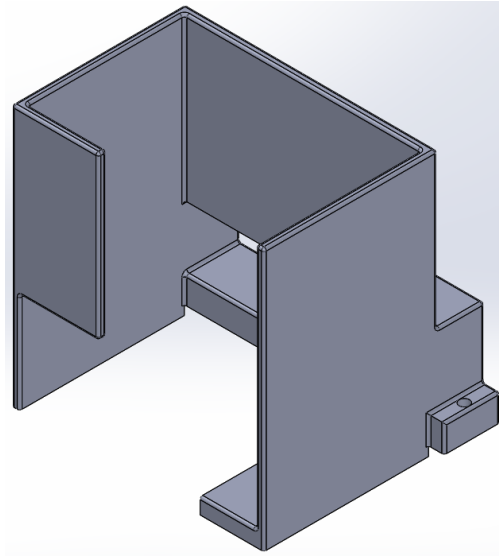


Figure 9: Belt Sander Casing

### 5.1.3 Work Cell Layout

The layout of the cell was mapped to ensure optimal functionality and efficiency. This involved considering various factors, including providing the vision system the required working range and field-of-view, positioning the belt sander at a considerable distance from the camera, and organizing the tool placement between the tray and gravity fixtures to its own section. This strategic arrangement was aimed at optimizing the overall workflow and spatial utilization within the work cell. By consolidating the tool placement to a quadrant, the available space was maximized, and the movement of the robotic arm between the tooling fixtures and belt sander was streamlined. This configuration not only enhanced the efficiency of tool handling but also facilitated smoother operations. It minimized the risk of collisions or obstructions as the manufacturing process flowed in a clockwise manner starting from the top left of the workspace if viewing head-on. Overall, these deliberate placement decisions contributed to the seamless functioning of the work cell, ensuring optimal performance and productivity (see Figure 10).

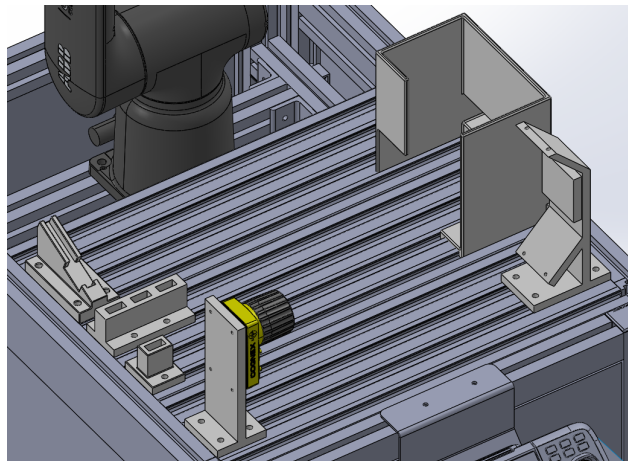


Figure 10: Iso View of Design Parts on Cart

## 5.2 Electrical Design

### 5.2.1 Load and Fuse Calculations

Prior to any wiring or electrical schematic mapping, load calculations were performed to ensure all device ratings were safely accounted for. In order to achieve this, the current drawing of all external devices were summed (see Table 1). As evident by Table 1, the total current draw from all external devices and components on the PLC panel was 8.06A. In efforts of cost savings, a spare Phoenix Contact UNO POWER 24VDC power supply was suitable as it was rated for a max output of 10A.

Table 1: Power Supply Device Current Ratings

Device Current Drawing	
Device	Current Draw (A)
PLC	2.30
Ethernet Switch	0.11
Belt Sander	5.00
Cognex Camera	0.50
Backlight	0.15
<b>Total</b>	<b>8.06 A</b>

While we can assure that the devices and electrical components will not overload the power supply's current rating, it was important to safeguard against potential surges in current draw during power cycles. To mitigate this risk, individual devices are equipped with fast-acting fuses. In this system, three fuses were utilized, rated for 3A, 5A, and 7A respectively. The 3A fuse is dedicated solely to the PLC, ensuring its protection. The 5A fuse safeguards the Cognex camera, backlight, and Ethernet switch. Meanwhile, the 7A fuse provides protection for the belt sander. These carefully selected fuses serve to safeguard the system's integrity and ensure uninterrupted operation.

### 5.2.2 Wiring Color

In the pursuit of designing an organized PLC panel, adherence to the National Electric Code (NEC) was prioritized in selecting wire colors [4]. This deliberate approach was adopted to minimize potential confusion and ensure clarity in the panel's wiring configuration for future maintenance and troubleshooting. Accordingly, the NEC electrical wiring code designates Black and Red as the primary and secondary hot wires, respectively. These distinct colors are visibly traced from and to the power supply, as well as to and from terminal blocks, facilitating the supply and return of 24VDC. Additionally, the selection of white and green wires were deliberate, with white signifying neutral and green symbolizing ground. Lastly, blue wires were strategically chosen to denote pathways exiting the PLC and extending into either relays or devices for I/O power distribution. This systematic approach to wire color selection not only enhances visual clarity but also streamlines the identification of wiring connections within the panel (See Figure X).

### 5.2.3 Component Selection

For the final phase of the electrical design, a comprehensive component list was curated, ensuring the system's readiness to distribute power to all devices effectively and safely (refer to Table 2). These components were selected with precision to meet the project's power requirements, ensuring seamless operation and compliance with safety standards. The creation of Table 2 also considered specific power and data cables essential for external devices, such as the Cognex camera and Moritex backlight, ensuring coverage of all electrical requirements for the system. In addition, given that the work cell was built on a modular cart,

it was imperative that the entire system required only one plug to operate. Since the cart already required power to operate the robot controller, a custom plug was designed to supply the power supply with the 120V it needed. The plug fit into an extra socket that the cart had. Through careful planning and consideration of each component's role and necessity, the electrical design phase culminated in the creation of a robust component list.

Table 2: Electrical Component list

Component List		
Component	Part NO.	Quantity
Power Supply	Phoenix Contact UNO POWER	1
PLC	Allen Bradley 5370 Compact Logix 1769 L16ER-BB1B	1
Ethernet Switch	Phoenix Contact FL Switch 1005N	1
AC Relay	Allen Bradley 700-HN104	1
DC Relay	Finder 34.5.1.7.024.0010	1
Fuse	Allen Bradley 1492-FB1C30-L	1
Fuse	Allen Bradley 1492-H	2
Terminal Blocks	Allen Bradley 1492-J3	14
M12 Female 8 Pin DB15	Lonlonty USLQ-5655	1
M12 Male 8 Pin A-Code RJ45	HangTon Connect M12A	1
M12 Female 4 Pin	uxcell a16110400ux0304J3	1
15-Amp 125-Volt 3-wire Plug	NEMA 4867-F-LW	1

## 5.3 Vision Design

### 5.3.1 Vision Environment

The vision environment was configured based off the criteria of providing optimal placement of the lens, positioned furthest away from the belt sander. In addition, this placement gave the the robot a centered position to hold the tool (see Figure 11. With the width of the table post-fixtature mounting being approximately 550mm, this location offered an ample working range for the equipment to operate effectively.

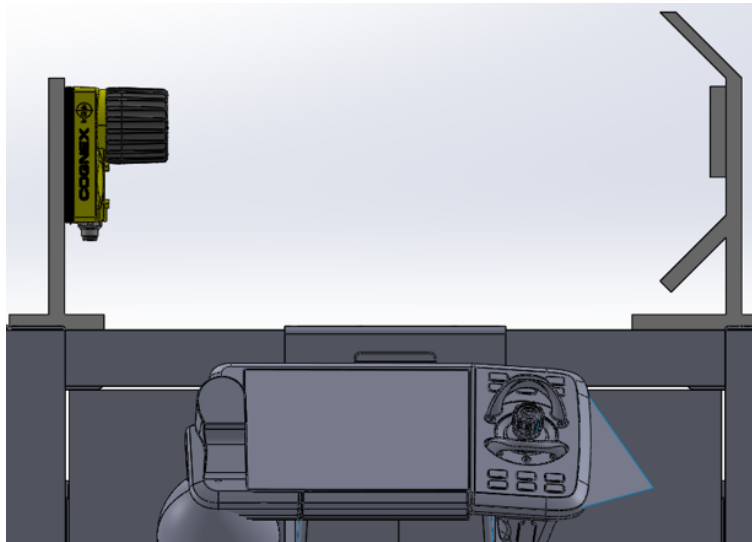


Figure 11: Vision Environment

### 5.3.2 Camera

The vision camera used in this system was the In-Sight 5100 Cognex Vision System, a loaner unit generously provided by Calvary Robotics, a local robotics integration company based in Webster, New York. The decision to opt for a Cognex camera stemmed from the compact footprint of the workcell. Cognex cameras, such as the 5000 series, are equipped with an embedded controller, eliminating the need for additional equipment and facilitating seamless integration with Allen Bradley PLCs. The selection of this specific camera model was made by the Vision team at Calvary Robotics, considering various factors. Given the application requirements, a camera without its own backlight was deemed sufficient. In addition, utilizing a Cognex Camera offered access to the In-Sight Explorer software, its proprietary software offering vision tools and machine image processing. The camera can be identified below:

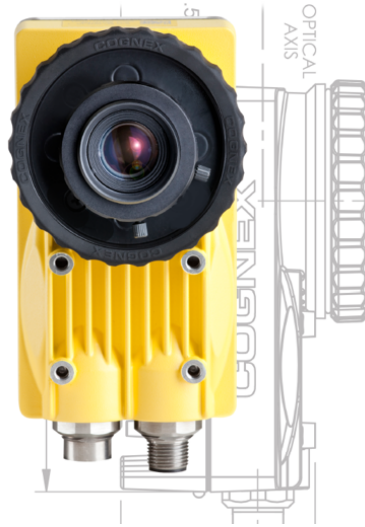


Figure 12: Cognex Camera

### 5.3.3 Lens

As for the lens, a 35mm lens was deemed appropriate by the 250mm working distance in which placed the tooling in the middle between the camera and the backlight. In addition, given that the desired field of view was relatively small and constrained to the edge of the tool, a lens with this small of a resolution was suitable for the task. The lens can be identified below:



Figure 13: HF35HA-1S Lens

### 5.3.4 Backlight

The backlight utilized was a Moritex CV-FL63X60B (see Figure 14a). This small backlight was suitable for the job due to its diffused light and ability to cover just the amount needed to view the tool's edge with the light behind it. Figure 14b demonstrates the ideal illumination structure placing the tool in front of the light between the camera and its lens.

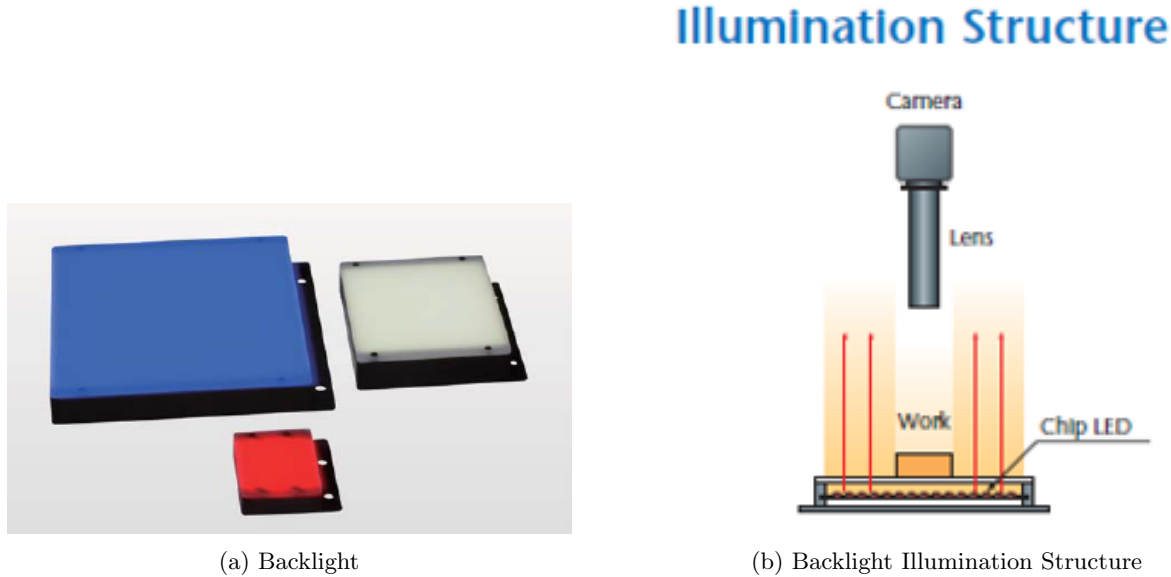


Figure 14: Moritex CV-FL63X60B Backlight

## 5.4 Design Decisions

### 5.4.1 Force Control

One crucial decision that required careful consideration was determining how the robot would detect when it had applied the necessary force/pressure to execute a 45° chamfer grind effectively. This detection method needed to be both calibrated and tested to ensure it consistently achieved the desired grind quality. Three potential methods were identified: acquiring the ABB Force Control License, which utilizes the torque sensors integrated into the individual joints of the CRB15000 robot; implementing an electro-mechanical End-of-Arm Tool (EOAT) equipped with force-detection technology; or incorporating a secondary vision system dedicated to detecting edge deflection of the EOAT. Each method offered its own set of strengths and weaknesses. A decision matrix, depicted in Figure 15, was employed to evaluate these methods. The ABB Force Control License emerged as the optimal choice, garnering the highest score of 11. Although it scored the lowest, the force control license demonstrated promising potential applications beyond the scope of this research, contributing to its selection.

Ranking				ABB Force Control License		EOAT Electro-Mechanical		Vision Camera	
1	Best	Criterion	Weight	Rank	Weighted Score	Rank	Weighted Score	Rank	Weighted Score
0.75		Force control Accuracy	5	1	5	0.5	2.5	0.75	3.75
0.5	Average	Robot Integration	4	0.75	3	0.5	2	0.5	2
0.25		Cost	3	0	0	0.5	1.5	0.25	0.75
0	Worst	Component Count	2	1	2	0	0	0.75	1.5
		Ease of Use	2	0.5	1	0.75	1.5	0.25	0.5
					11		7.5		8.5

Figure 15: Force Control Decision Matrix



### 5.4.2 Belt Sander

Given the small footprint of the tools, particularly the dimensions of 3" x 1" x 3/8", the selection criteria for the belt sander were relatively straightforward. The main focus was to find a sander that could accommodate similar-sized objects and perform grinding tasks typically associated with knife and jewelry work. After conducting thorough research, a belt sander meeting these requirements was identified (see Figure 16). This model offered adjustable power settings ranging from 12 to 24V, making it suitable for the intended application and ensuring compatibility with the small-scale tools to be grounded.

<b>SPEED MODE</b>	7-SPEED ADJUSTMENT
<b>MOTOR MATERIAL</b>	ALL COPPER MOTOR
<b>BODY MATERIAL</b>	304 STAINLESS STEEL
<b>MOTOR</b>	DUAL OUTPUT SHAFT 775
<b>VOLTAGE</b>	110V(US PLUG)
<b>RATED VOLTAGE</b>	12-24V
<b>ROTATING SPEED</b>	4000-8000RPM
<b>BELT SIZE</b>	330*30MM (13 IN X 1.2 IN)

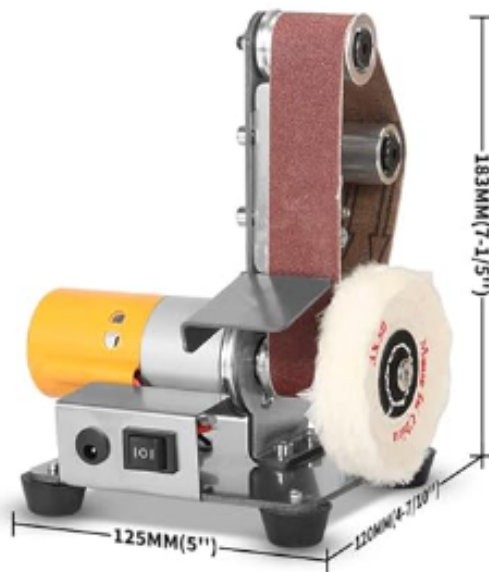


Figure 16: Belt Sander

## 6 Build Phases

### 6.1 Mechanical Build Phase

#### 6.1.1 Additive Manufacturing

All fixtures intended for mounting on the T-slot aluminum extrusion workspace atop the cart were chosen to be 3D printed to achieve cost savings. The Bambu Lab X1 Carbon and Ultimaker S7 printers were utilized for printing these fixtures, as they provided sufficient tolerancing for the print requirements (see Figure 17). Additionally, Polylactic Acid (PLA) was selected as the printing material due to its optimal balance between cost-effectiveness and stability required for the parts. Once the fixtures were printed they were mounted to the cart's top by 18-8 Stainless Steel, M8 x 1.25 mm Thread, 35mm Long Hex Bolts secured by a T-slotted nut.



(a) Bambu X1 Carbon



(b) Ultimaker S7

Figure 17: 3D Printers Used

#### 6.1.2 Fabrication

During the project, two things required machine fabrication and the use of the Machine Tools Lab located within RIT. The first was the base plate of the belt sander. Given that the belt sander will be activated and will be undergoing force by the tool pressing against it, it was important that it could be mounted to the table in a position that would restrict it from deflecting and moving when exhibiting the force from the tool being pressed against it and while the motors on. In order to do this, 2 M8 clearance holes were placed on the plate 45mm apart. This was done using a Bridgeport Mill (see Figure 18).

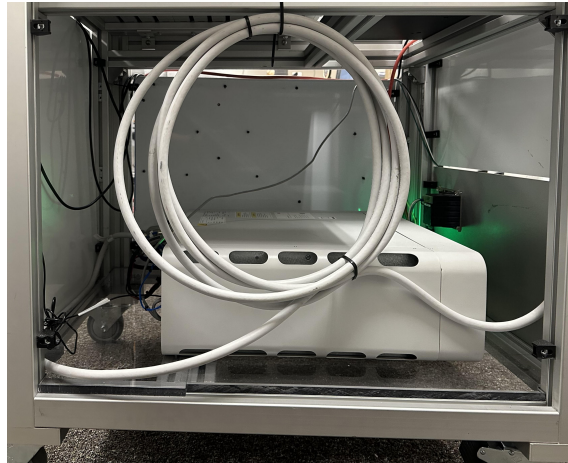


Figure 18: Belt Sander Baseplate on Mill

Another component that underwent fabrication was the PLC panel. With the goal of ensuring modularity within the work cell, the panel needed to be adaptable for mounting on the side of the cart. This involved removing one of the side panels and mount the metal panel that would house the DIN rails and electrical components, aligning it with the dimensions of the mounting holes (see Figure 19a). The four mounting holes on the side panels were spaced 28" by 18" apart (see Figure 19b). By accounting for these dimensions and adding a quarter inch on each side of the panel, the panel was precisely cut using a band saw. Subsequently, the M7 holes were drilled into the panel at their respective locations using a drill press. Following fabrication the panel was mounted and in position to begin assembly and wiring. Figure 20 demonstrates how to old panel looked prior to cutting and drilling the new mounting holes in it.



(a) Original Side Panel on Cart



(b) Side Panel Taken Off

Figure 19: Side Panel of Cart

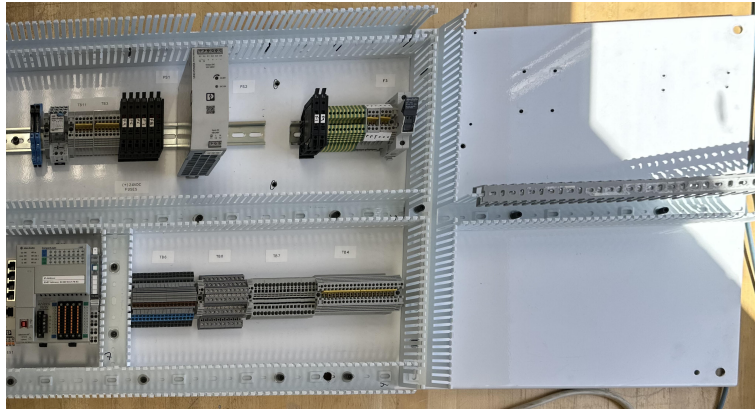


Figure 20: Old Panel Before Cutting and Mounting Holes

The final stage of fabrication involved cutting the raw 6061 aluminum stock into the specified tool dimensions. Initially, the raw stock, conveniently sized at 3 feet in length with a width of 1 inch and a thickness of  $3/8$  inch, was prepared for processing. To achieve precise cuts, the material was transported to the Brinkman Laboratory within the Kate Gleason College of Engineering, where it was loaded into an auto feeder CNC cutter in which returned the desired 3 inch tool samples. This CNC machine enabled accurate and consistent cuts, resulting in the production of over 110 test samples. Figures 21a and 21b visually depict an individual ungrounded tool and the raw stock material, respectively, highlighting the outcomes of the fabrication process.



(a) Individual Ungrounded Tool



(b) Raw Stock

Figure 21: Tool Samples



## 6.2 Electrical Build

### 6.2.1 PLC Panel Wiring and Layout

The PLC panel was constructed using four separate DIN rails arranged across two levels, with dimensions of 16.5", 6.5", 7.5", and 17.5". This configuration allowed for the incorporation of intermediate vertical raceways between two DIN rails on each level, in addition to the horizontal ones between DIN rails and others surrounding the edges of the panel. The inclusion of these raceways significantly improved cable management by providing additional paths for wires to flow, thereby reducing redundant wiring paths and ensuring a more robust flow of wiring throughout the panel (refer to Figure 22). Power is supplied to the panel through a custom-built plug designed to connect a hot, ground, and neutral wire, which then plugs into the socket located at the back of the cart (refer to Figure 23).

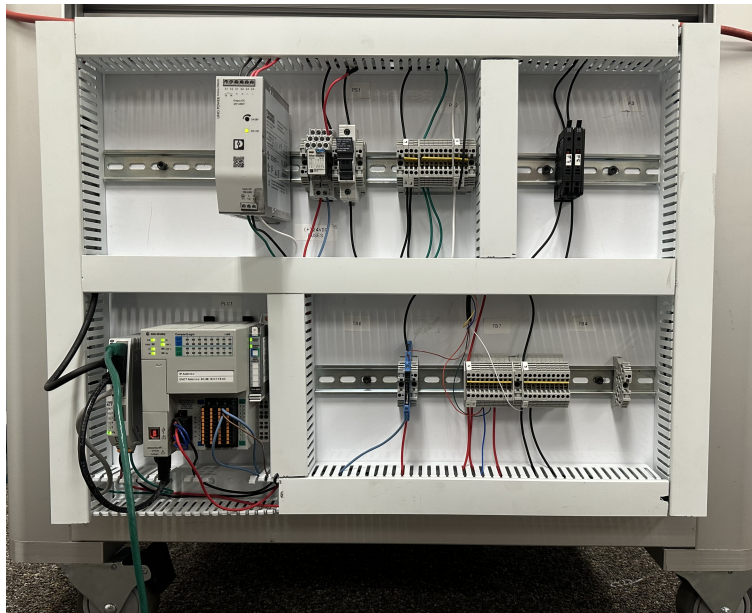


Figure 22: Fully Built, Wired, and Mounted PLC Panel



Figure 23: Custom-built Plug

### 6.2.2 External Device Wiring

The three primary external devices included the 5100 In-Sight Cognex Camera, the SI-Fang Electric Belt Sander, and the Moritex CV-FL-63x60B-M12 backlight. Each device presented unique pin-out diagrams that required careful adherence to ensure proper wiring to the PLC panel. For instance, the Cognex camera relied on an M12 8-pin connector for its 24VDC power supply, as illustrated in Figure 24. Notably, only four of the pins were utilized for our specific application: Pin 1 for +24VDC, Pin 2 for Trigger+, Pin 3 for Trigger-, and Pin 8 for 24V Common. Pins 4-7 remained unused, reserved for other cameras and communication protocols beyond Ethernet/IP. To leverage the trigger function effectively, Trigger+ was connected through a DC relay in a normally open (NO) configuration, enabling its closure when a trigger for image capture was initiated.

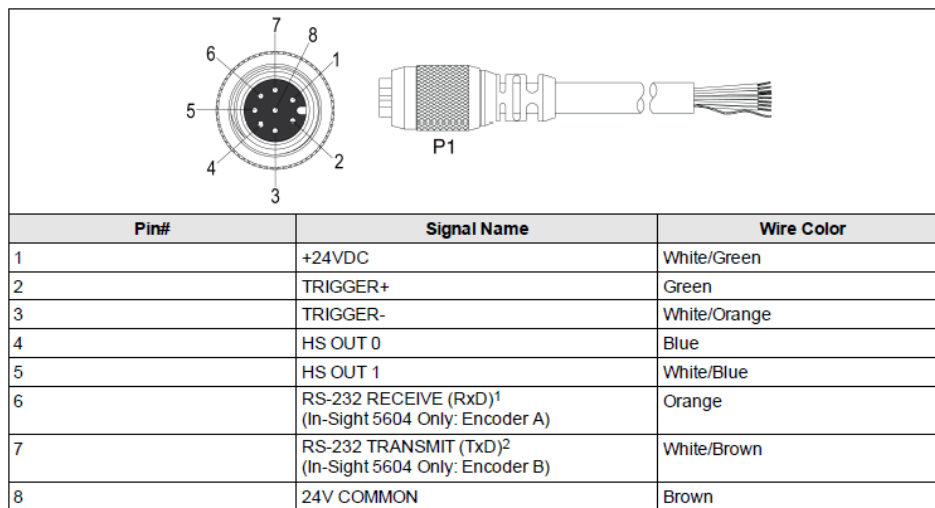


Figure 24: Cognex Camera Pin-out Diagram

The Moritex backlight utilized an M12 4-pin connector for its power supply, as illustrated in Figure 25. The pin-out configuration consisted of Pin 1 for V+, Pin 2 for NC (Normally Closed), Pin 3 for V-, and Pin 4 for NC. Since the functionality of the light was binary—simply needing to be turned on or off—it was directly wired to the PLC. In this setup, power was either supplied or withheld based on the operational requirements at any given time. As for the belt sander, it was a simple dual-polarity wire. The sander was cut at the plug end and the wire was stripped to run through an AC relay in a normally open (NO) configuration. This allowed for the AC motor to remain off, but actuate based on when signal was supplied from the discrete I/Os on the PLC.

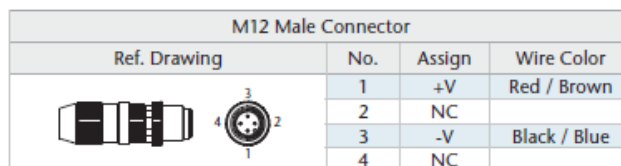
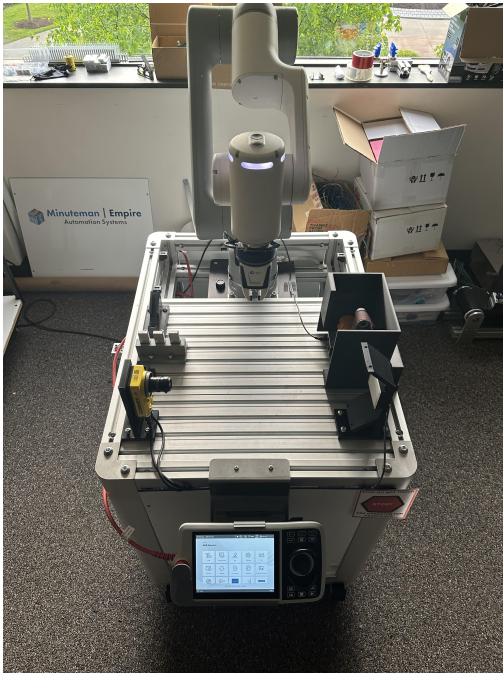


Figure 25: Moritex Backlight Pin-out Diagram

### 6.3 Fully Assembled Cell

Figures 26a and 26b display the full assembled workcell with all electrical and mechanical components completed



(a) Top View of Fully Assembled Workcell



(b) Iso View of Fully Assembled Workcell

Figure 26: Tool Samples



# 7 Software Deployment

## 7.1 Network Design

To ensure effective communication among the networked devices, a robust protocol needed to be established and configured. Ethernet/IP was chosen as the communication protocol for this application. The network was set up using the Class C IPv4 address space, with the address "192.168.125" designated for device communication. Each device was assigned a unique host address in the last octet. As for the subnet mask, the "255.255.255.0" was employed to define the network boundaries.

While the PLC possessed the capability to serve as the central processing unit for initiating the grinding procedure, this responsibility was delegated to the Omnicore controller. Instead, the PLC functioned as a continuously operational remote I/O block, ready to facilitate communication and data transfer between devices. It responded promptly to I/O signals raised high or low, as dictated by the robotic program, ensuring seamless coordination across the system's devices. Figure 27 demonstrates how each device is configured on the network, as well we which device is the MCP of the network.

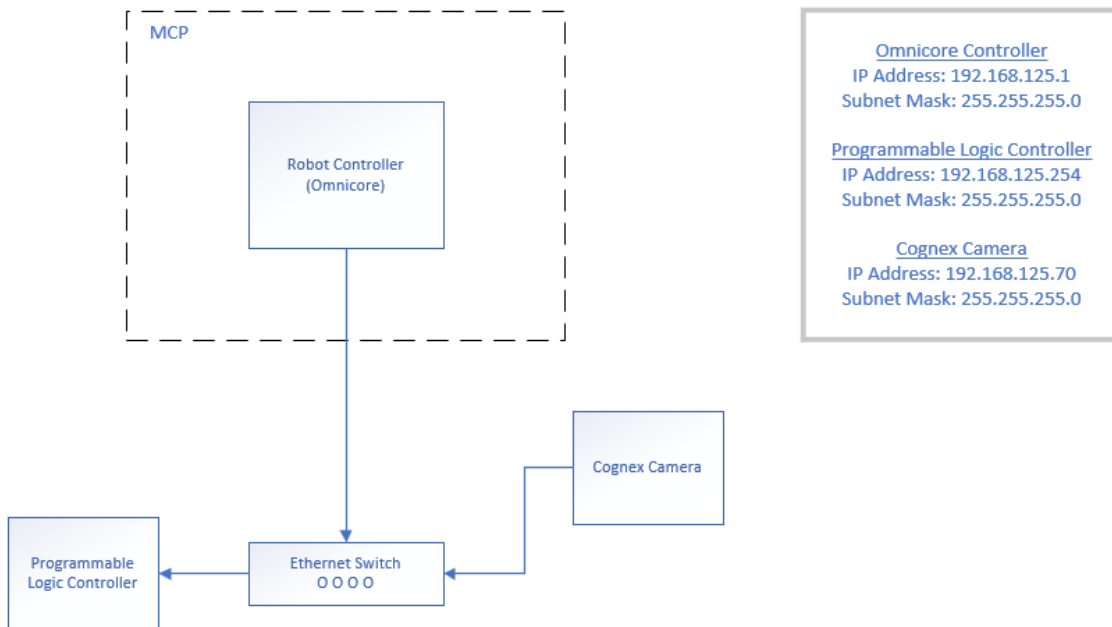


Figure 27: Network Overview

## 7.2 PLC

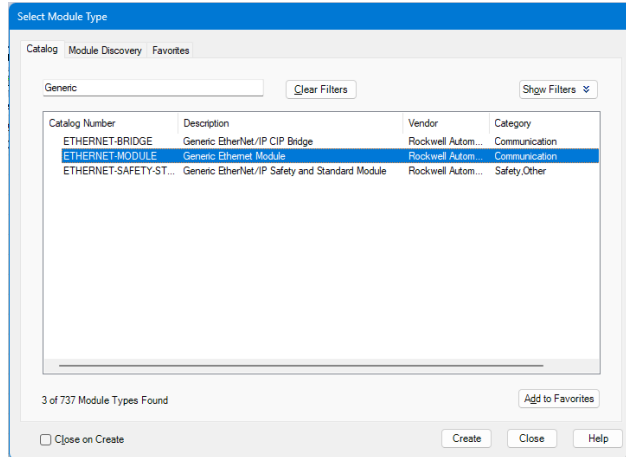
The PLC utilized for this system is a 1769-L16ER-BB1B Compact Logix 5370 controller. The PLC is designed with Embedded Discrete I/Os and is to be programmed using Studio5000 Logix Designer v32.04.00.

### 7.2.1 Generating Device Modules

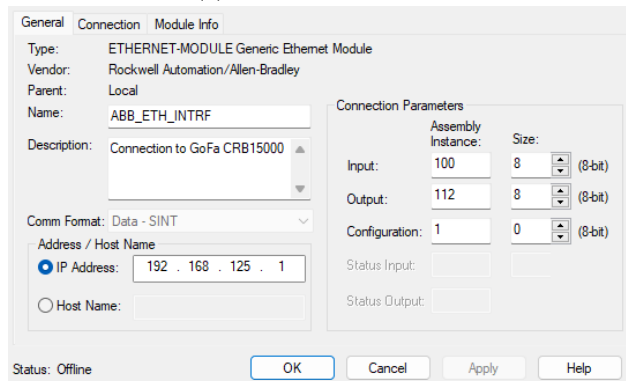
Once the PLC is online and talking to the computer, modules for the devices that wish to communicate over Ethernet/IP can be generated. The Connection Parameters of a device can be found in their respective manual. or an Omnicore controller using RobotWare 7, the Connection Parameters can be found in the ABB

Ethernet/IP Scanner/Adapter Application Manual [1]. The following instructions will show how to setup a new module within Logix Designer:

- Right click "Ethernet" in Controller Organizer panel → New Module → Search "Generic" → Select "Generic Ethernet Module" (see Figure 28a) → Enter device's IP and Connection Parameters (see Figure 28b)



(a) Select Module Type



(b) Defining Module

Figure 28: Creating New Module (Steps for Adding ABB)

In specific cases, an Add-On Profile (AOP) can be downloaded to facilitate seamless integration via Ethernet/IP. Cognex, for instance, provides an AOP on their website tailored for Studio 5000 applications aiming to interface with In-Sight Explorer firmware [5]. Upon download, this AOP seamlessly installs and configures within Studio 5000 automatically incorporated into the catalog (see Figure 29).

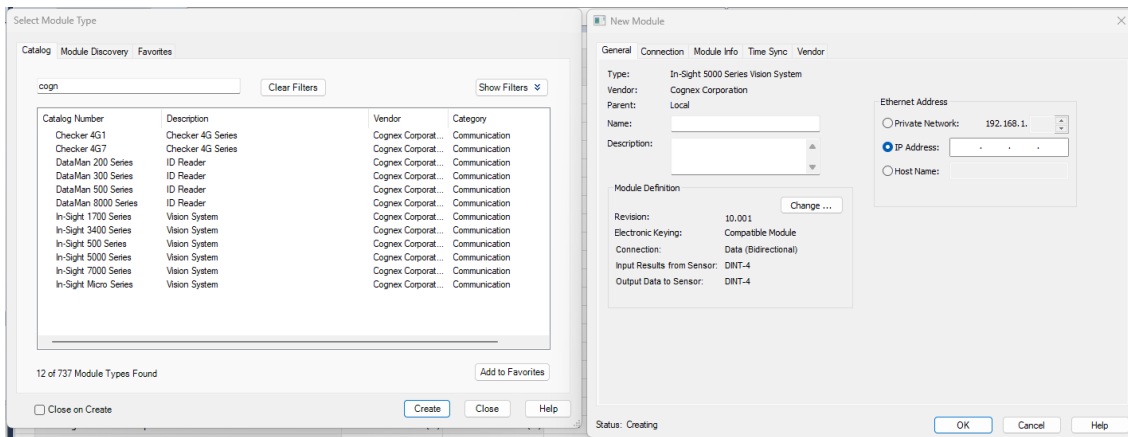


Figure 29: Creating a Cognex Module

## 7.2.2 Create Local Tags

Once the modules are created in the Logix Designer, the local tags for the devices can be created. These tags are to serve as the alias mapping component to the desired output boolean bit that is to be energized when the device is required to turn on. These local tags pertain solely to the belt sander and backlight as those are configured to be normally open seeking a closed contact to turn on. The process of defining these tags is as follows:

- Right click "Controller Tags" in Controller Organizer panel → "New Tag" → Change Type to "Alias" → Change "Alias For" to corresponding output in which device was wired to the PLC's embedded digital output (see Figure 30) → Change Data Type to "BOOL" → "Create"

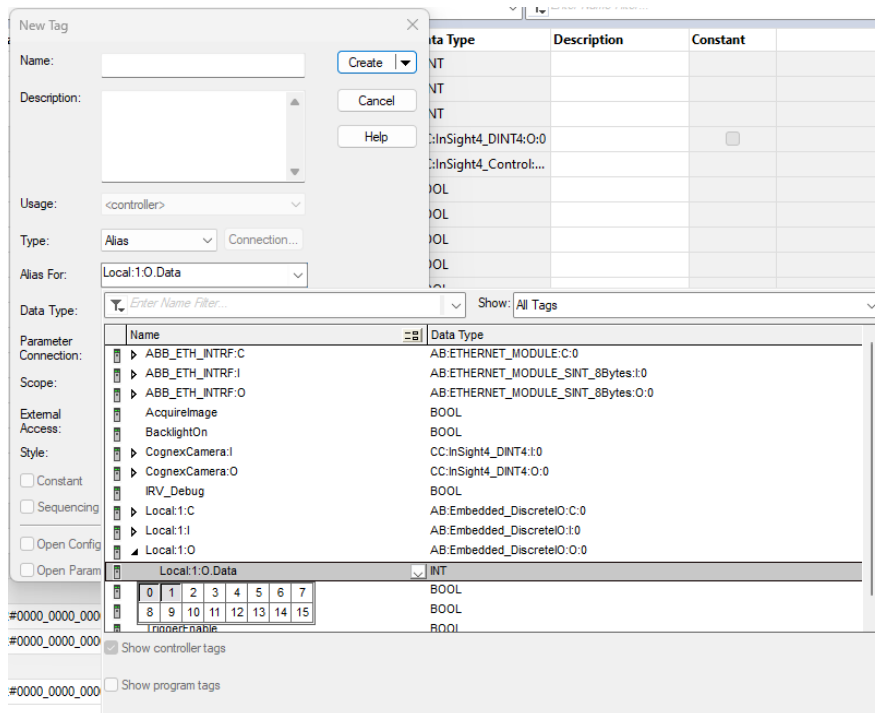


Figure 30: Creating a Local Tag

Device tags were also required in order to facilitate communication between the PLC and the respective equipment. Created similarly to Local Tags, these are controller tags in which are mapped to the respective I/O configured within RobotStudio (see Figure 31)

BacklightOn	ABB_ETH_INTRF:l.Data[0].1	ABB_ETH_INTRF:l.Data[0].1	BOOL
▶ CognexCamera:l			CC:InSight4_DINT4:l:0
▶ CognexCamera:O			CC:InSight4_DINT4:O:0
IRV_Debug			BOOL
▶ Local:l:C			AB:Embedded_Discr...
▶ Local:l:l			AB:Embedded_Discr...
▶ Local:l:O			AB:Embedded_Discr...
RobotCallsTrigger	ABB_ETH_INTRF:l.Data[0].2	ABB_ETH_INTRF:l.Data[0].2	BOOL
SanderOn	ABB_ETH_INTRF:l.Data[0].0	ABB_ETH_INTRF:l.Data[0].0	BOOL

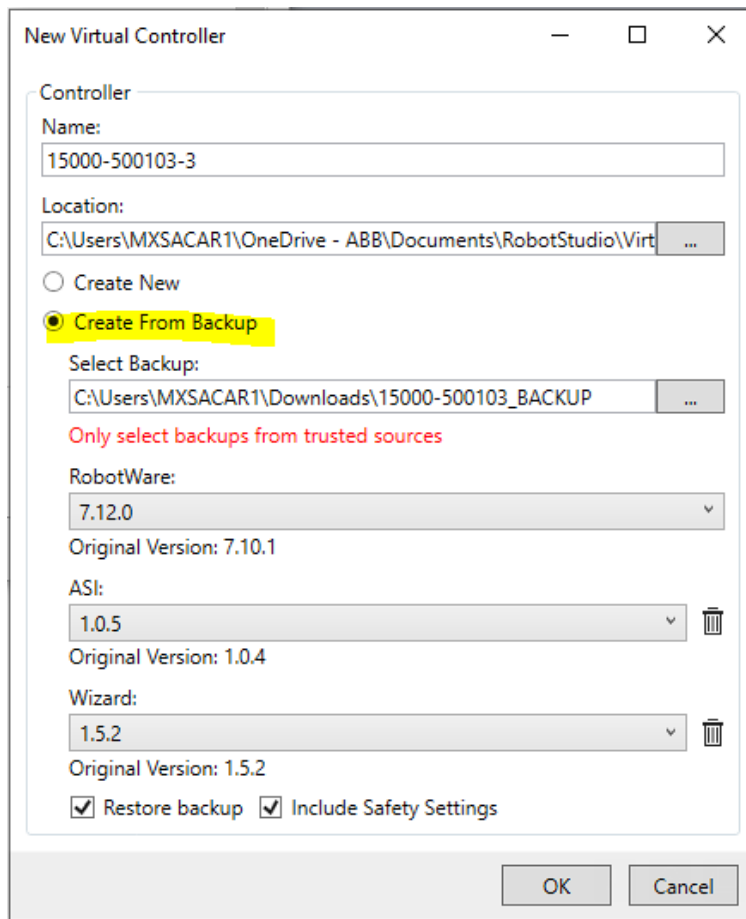
Figure 31: All Created Device and Local Tags

Once the tags were created, the required Ladder Logic was constructed. It is important to note that the PLC in this system was designed to act as remote I/O block and not the main control point. What this meant is that it is not responsible for initiating the procedure but instead was running continuously waiting for signals from the robot controller or the Cognex Camera to perform the required task whether that be turn on an external device (belt sander and backlight), trigger the camera, or transfer the angle result from the camera to the robot's controller (see Appendix XXX for the complete PLC program).

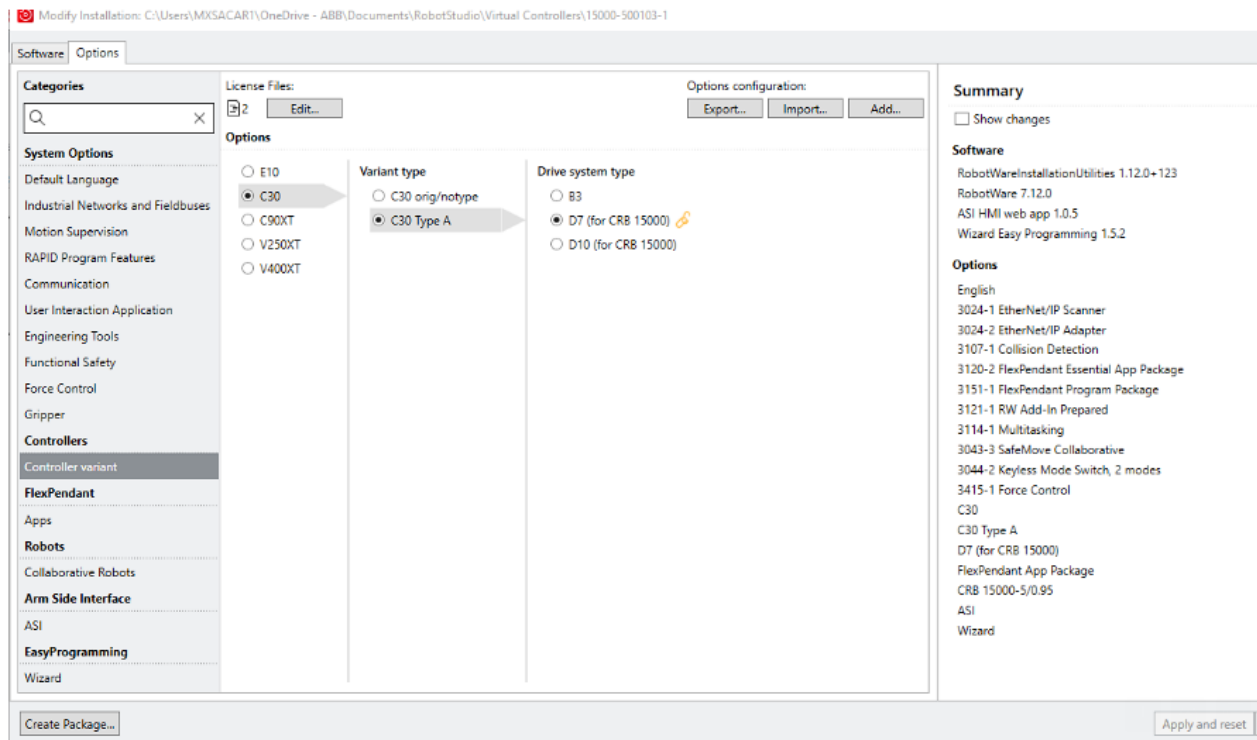
## 7.3 Robotic Integration

### 7.3.1 Robotic Controller Configuration

The first step to integrating the CRB15000 robot to the workcell was configuring its physical controller. The Omnicore C30 is the controller was the robot's central processing unit, responsible for storing and executing all related procedures and tasks. Configuring this controller came with challenges as the original controller did not have the Force Control license which was the elected method of executing the grind method for this application. To activate the Force Control License, several steps were initiated. Initially, a new virtual controller was established within Robot Studio to accommodate the uploaded license. Concurrently, RobotWare 7.12 was integrated into the newly created controller to ensure seamless compatibility with the Force Control feature (see Figure 32a and 32b). This integration necessitated a full system restart, facilitating the seamless transfer of the license onto the physical controller.



(a) Creating New Virtual Controller



(b) Modifying Installation

Figure 32: Configuring Force Control

Following the license activation process, a Cyclic Break Check was executed to verify the functionality of the robot's joints. This verification was conducted using the Teach Pendant, as well as a new SafeMove Safety Configuration. The purpose of the Safety Configuration is to establish a predefined safe zone within which the robot can operate safely. This was defined to a region that mapped the cart's footprint with an additional foot on each side.

### 7.3.2 Data Types

Once the controller was configured with the Force Control license, global data types were established (see Figure 33). Taught manually on the Teach Pendant the following data types were created:

- Tool Center Point (TCP)
  - A TCP provides a coordinate system at the functional end of the EOAT that is used. Given that a gripper EOAT is being used, the base "tool0" TCP does not accurately represent the distal end of the robotic arm. Failure to define a new TCP with any EOAT will provide inaccurate positional data come time for the robot to interact with the environment or performs tasks.
- Work Objects (WObj)
  - A Work Object is a local coordinate system within the robot's workspace where tasks are performed. It serves as the reference point for the robot's movements and operations. Properly defining the work object is crucial for ensuring accurate and efficient task execution.
- Robot Targets (Robtarget)
  - Robtargets are predefined positional points in a robot's workspace that represent a specific location. These targets serve as reference points for the robot to move to during its operations. Robtargets allow for precise positioning and orientation of the robot's end-effector relative to the work object or coordinate system it was defined within.
- Load Data
  - Load data encompasses payload details like weight, dimensions, and center of gravity. It enables the controller to optimize motions, ensuring safe and efficient operation while interacting with the payload. This is crucial for the tool grinding application, as it enables the Force Control sensors to exert a more accurate force when requested.

```
TASK PERS tooldata tGripper := [TRUE,[[4.39225,2.26359,169.311],[1,0,0,0]],[0.7,[16.7,28,74],[1,0,0,0],0,0.011,0]];
PERS loaddata loadGT :=[0.5,[-50.4,-19.6,-87.3],[1,0,0,0],0,0,0,0];

TASK PERS wobjdata wobjTray :=[FALSE,TRUE,"",[[373.7853,-184.158,124.2313],[0.0003937004,0.003477711,0.001236416,-0.9999931]],[[0,0,0],[1,0,0,0]];
TASK PERS wobjdata wobjSander := [FALSE,TRUE,"",[[397.8671,203.356,127.5784],[0.7070533,0.01288801,-0.001513496,0.7070411]],[[0,0,0],[1,0,0,0]];
TASK PERS wobjdata wobjGrav1 := [FALSE,TRUE,"",[[320.2415,-268.9555,134.333],[0.005571439,-0.2024923,-0.01569495,-0.9791422]],[[0,0,0],[1,0,0,0]];
TASK PERS wobjdata wobjGrav2 := [FALSE,TRUE,"",[[463.7106,-259.4765,123.716],[0.0003307542,-0.003525678,0.001478235,0.9999926]],[[0,0,0],[1,0,0,0]];

CONST jointtarget jpHome := [[0,-30,60,0,60,150],[9E+09,9E+09,9E+09,9E+09,9E+09,9E+09]];
CONST robtarget pSampleR :=[[25.51,18.66,-2.18],[0.0178847,0.868545,-0.495263,-0.00480767],[-1,0,0,0],[9E+09,9E+09,9E+09,9E+09,9E+09,9E+09]];
CONST robtarget pSampleC :=[[25.52,58.34,-2.18],[0.0178861,0.868546,-0.495262,-0.00480802],[-1,0,0,0],[9E+09,9E+09,9E+09,9E+09,9E+09,9E+09]];
CONST robtarget pSampleL :=[[25.54,97.13,-2.20],[0.0178919,0.868533,-0.495284,-0.00478814],[-1,0,0,0],[9E+09,9E+09,9E+09,9E+09,9E+09,9E+09]];
CONST robtarget pGravDrop := [[71.56,9.12,-27.35],[0.569502,0.198973,-0.784316,-0.144658],[-1,0,0,0],[9E+09,9E+09,9E+09,9E+09,9E+09,9E+09]];
CONST robtarget pGravPick := [[36.64,7.42,-63.73],[0.0274547,0.275331,-0.960952,-0.00316467],[-1,-1,1,0],[9E+09,9E+09,9E+09,9E+09,9E+09,9E+09]];
CONST robtarget pGrindLeft := [[31.1,24.6,72.86],[0.0977089,0.892494,0.233356,0.373433],[0,0,0,0],[9E+09,9E+09,9E+09,9E+09,9E+09,9E+09]];
CONST robtarget pInspect := [[568.46,54.04,215.26],[0.137665,0.806499,0.219961,0.531248],[0,0,1,1],[9E+09,9E+09,9E+09,9E+09,9E+09,9E+09]];
CONST robtarget pGravDrop2 := [[27.44,10.69,52.60],[0.611956,0.620809,-0.339482,0.353353],[-1,0,-1,0],[9E+09,9E+09,9E+09,9E+09,9E+09,9E+09]];
CONST robtarget pGravPick2 := [[25.95,23.39,-1.64],[0.0160083,-0.877571,0.47917,0.00314492],[-1,-1,0,0],[9E+09,9E+09,9E+09,9E+09,9E+09,9E+09]];
CONST robtarget pPlaceR := [[25.94,21.97,34.67],[0.0183399,-0.873166,0.487056,0.00466829],[-1,-1,0,0],[9E+09,9E+09,9E+09,9E+09,9E+09,9E+09]];
CONST robtarget pPlaceC := [[25.88,61.33,33.81],[0.0183456,-0.873147,0.487089,0.00464979],[-1,-1,0,0],[9E+09,9E+09,9E+09,9E+09,9E+09,9E+09]];
CONST robtarget pPlaceL := [[25.57,100.61,33.33],[0.0183457,-0.873132,0.487116,0.00462506],[-1,-1,0,0],[9E+09,9E+09,9E+09,9E+09,9E+09,9E+09]];

```

Figure 33: Globally Defined Data Types

### 7.3.3 I/O Configuration

In order to program a complete RAPID procedure, the desired I/O system must be configured. These included the Scalable I/Os in which facilitated the manipulation of the electric gripper, as well as the I/Os that will allow for actuation of the external devices (belt sander, Cognex Camera, backlight) over Ethernet/IP. Detailed instructions for configuring the Scalable I/Os can be found in the ABB Scalable I/O Application Manual [2] As per defining the I/Os for the actuation of the external devices, this was done via a signal creation within RobotStudio.

- Controller → Configuration → I/O System → Signal (Right Click)

This opens up the Instance Editor where the signal name, type, device assignment, category, and access level can be defined (see Figure 34 . It was important that the device assignment for these I/Os were assigned to "EN\_Internal\_Device" as this configured it to the Ethernet/IP. Through this setup, the following I/O were created:

Digital Outputs:

- doBacklight (Backlight)
- doCognexTrigger (Camera Trigger)
- doSander (Belt Sander)

Group Inputs:

- GIGrindAngle (Detected Angle)
- GIByte0 (Debug I/O)

Name	Value	Information
Name	doBacklight	
Type of Signal	Digital Output	
Assigned to Device	EN_Internal_Device	
Signal Identification Label		
Device Mapping	1	
Category		
Access Level	All	
Default Value	0	
Invert Physical Value	<input type="radio"/> Yes <input checked="" type="radio"/> No	
Safe Level	DefaultSafeLevel	

**Value (RAPID)**  
The changes will not take effect until the controller is restarted.  
Minimum number of characters is <invalid>. Maximum number of characters is <invalid>.

OK Cancel

Figure 34: Defining New I/O

### 7.3.4 RAPID Procedures

With the I/Os fully configured and the PLC receptive of them all, the complete RAPID procedure could be written. This is the robotic program in which will be executed to complete the complete grinding procedure of the three tools. This portion was devised into sub procedures that complete specific portions of the procedure such as the grinding portion, angle inspection, and tool placement between fixtures. By defining smaller sub-procedures they can all be referenced in the main procedure which is what the robot executes (see Figures 35).

```
PROC Grind()
    MoveJ Offs(pGrindLeft,-5,0,0),v30,fine,tGripper\WObj:=wobjSander;
    SetDO doSander, 1;
    WaitTime .5;
    MoveL pGrindLeft,v30,fine,tGripper\WObj:=wobjSander;

    InitialToolPosition := CRobot(\Tool:=tGripper\WObj:=wobjSander);
    InitialX := InitialToolPosition.trans.x;

    IFCSetDampingTune xdamp, ydamp, zdamp, rxdamp, rydamp, rzdamp;
    FCPressLStart pGrindLeft, v30, \Fx:=3, 75, \ForceFrameRef:=FC_REFFRAME_WOBJ, \ForceChange:=20, \PosSupvDist:=1000, fine, tGripper\WObj:=wobjSander;

    WHILE CurrentX - InitialX < 2.5 DO
        FCPressL Topoint := Offs(pGrindLeft,2,0,-1),v5,Fx,fine,tGripper\WObj:=wobjSander;
        WaitTime .5;

        CurrentGrindPos := CRobot(\Tool:=tGripper\WObj:=wobjSander);
        CurrentX := CurrentGrindPos.trans.x;
        WaitTime .5;

    ENDWHILE

    CurrentX := 0;
    FCPressEnd Topoint := Offs(pGrindLeft,-5,0,0),v10,tGripper\WObj:=wobjSander;

    SetDO doSander, 0;
    MoveJ Offs(pGrindLeft,-30,0,0),v30,z200,tGripper\WObj:=wobjSander;
ENDPROC
```

(a) Grind Sub Procedure

```
PROC AngleInspection()
    MoveJ pInspect,v50,fine,tGripper\WObj:=wobj0;
    SetDO doBacklight, 1;
    WaitTime 1;
    PulseDO doCognexTrigger;
    WaitUntil GInputdnum(GIGrindAngle) > 0;
    SetDO doBacklight, 0;

    nGrindAngle := (GInputdnum(GIGrindAngle))/1000;
    sGrindAngle:=dnumToStr(nGrindAngle,3);
    TPWrite sGrindAngle;
ENDPROC

PROC Pick2Grind(robtarget pSampleL)
    MoveJ Offs(pSampleL,0,0,200),v100,z50,tGripper\WObj:=wobjTray;
    MoveL pSampleL,v50,fine,tGripper\WObj:=wobjTray;
    closeGripper;
    WaitTime .5;
    MoveL Offs(pSampleL,0,0,200),v100,z50,tGripper\WObj:=wobjTray;

    GravFixture1;
    Grind;
ENDPROC

PROC Inspect2Place(robtarget pPlaceL)
    AngleInspection;
    GravFixture2;

    MoveJ Offs(pPlaceL,0,0,200),v100,z50,tGripper\WObj:=wobjTray;
    MoveL pPlaceL, v10,fine,tGripper\WObj:=wobjTray;
    openGripper;
    WaitTime .5;
    MoveL Offs(pPlaceL,0,0,200),v100,z50,tGripper\WObj:=wobjTray;
ENDPROC
```

(b) Other Sub Procedures

Figure 35: Sub Procedures

Examining the Grind subroutine in Figure 35a in greater detail, the Force Control aspect of the project is exhibited. The pseudo-code entails the application of a 3N force in the X direction at a velocity of 30 mm/s to the belt sander. This force underwent meticulous refinement through iterative experimentation, primarily aimed at preventing the tool from slipping out of the gripper's jaws during operation. Initially,



this presented a significant challenge due to insufficient friction between the gripper and the aluminum tool. To address this challenge, adjustments were made to the gripper's pickup position from the ramped gravity fixture. By positioning it closer to the intended grinding edge, the moment experienced by the tool upon contact with the belt sander was effectively reduced. Additionally, modifications were implemented in the robotic path, ensuring that the sander was approached at a downward angle aligned with the direction of its rotation (see Figure 36).

Furthermore, the means in which the procedure was programmed such that it can meet a conditional requirement that satisfies the required grind is given by the While Loop developed. The While Loop details that so long as the X position of the robot has not changed by 2.5mm, the force will continue to be apply. It is important to note that this 2.5mm does not mean that 2.5mm was grounded off the tool's edge, but instead takes into account the deflection that the belt sander undergoes as the force is applied on the tool. These strategic refinements not only optimized the grinding process but also mitigated the risk of slippage, thereby facilitating precise and efficient grinding operations. Once the sub-procedures were defined, the Main procedure could be written in which calls these subroutines in the respective order that completes the successful grind of the three tools.

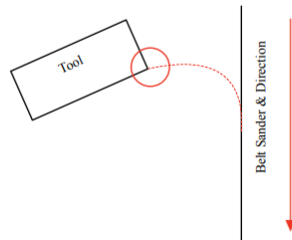


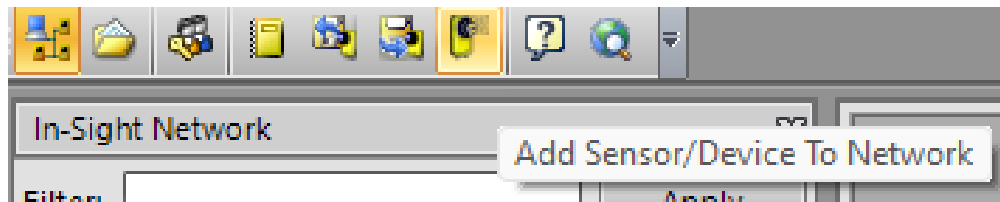
Figure 36: Tool Grind Path

## 7.4 Vision Integration

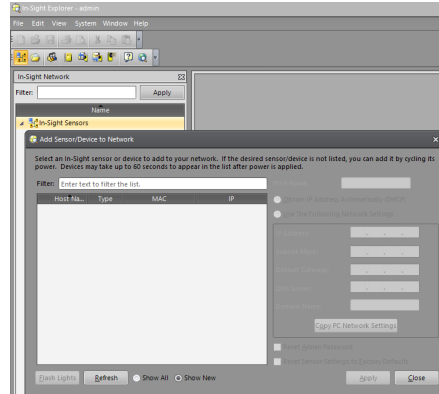
### 7.4.1 Connecting to Camera

Leveraging Cognex's In-Sight Explorer software, connection to the camera was seamless. Once the camera is added to the network, images can now be taken and the vision processing section can begin. The following instructions provide the context of how to add the camera to the network:

- Click the Camera Icon (see Figure 37a → click respective camera listed in window → configure I/P address of the camera → Click "Apply")



(a) Adding Camera to Network



(b) Configuring Camera's IP

Figure 37: Adding Camera to Network

#### 7.4.2 Image Processing

Once the camera was online, fine tuning of its aperture and focus rings can be completed to provide optimal resolution, depth of field, and overall image sharpness. This was then further improved through the adjustment of its exposure within the In-Sight Explorer software. Once the desired image settings were configured, an image can be captured and the processing may begin.

In this machine vision application, the primary objective was to detect angles, eliminating the need for pixel-to-millimeter calibration. Instead, the approach focused solely on pattern matching and edge detection to acquire the necessary data for angle computation. The taught pattern centered on the grounded edge. Figure 38a showcases the pattern integrated into the system, while Figure 38b illustrates the corresponding search region. These visual representations are critical as they empower the vision system to accurately detect the overall area and feature of interest.

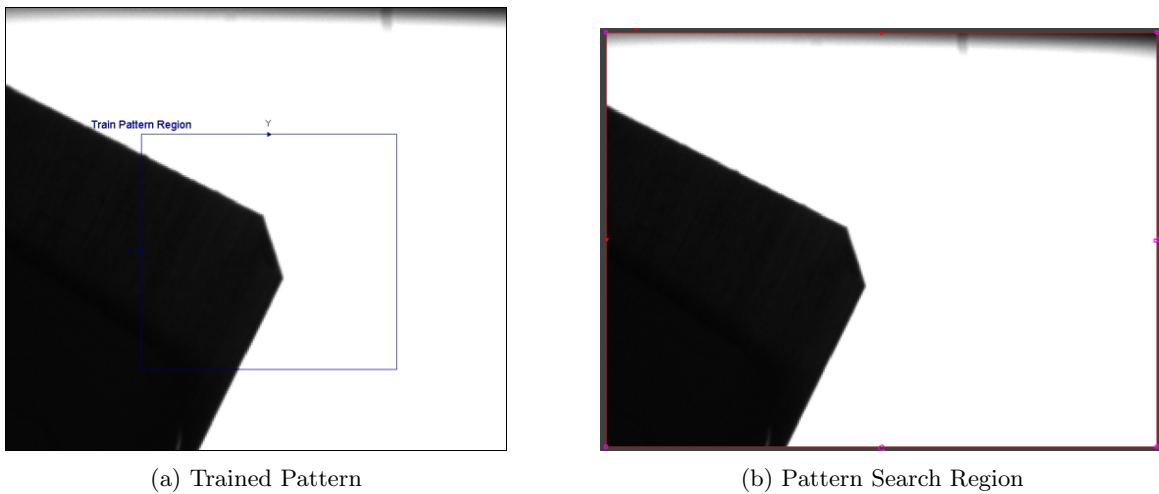


Figure 38: Image Pattern Training

After teaching the pattern, the next step involved teaching the edges necessary for angle computation. This entailed identifying both a straight edge and a grounded edge, facilitating the utilization of the "GetAngle" function within the In-Sight Software. Figure 39a was initially taught as the straight edge against which the grounded edge would be compared for angle computation. It was crucial to train this edge in a configuration where the bounding box aligned parallel to the tool's straight edge. Similarly, it was imperative for the bounding box of the grounded edge, as depicted in Figure 39b, to be parallel the actual grounded edge of the tool. Furthermore, it was essential for the coordinate directions of these bounding boxes to align in such a manner that the grounded edge's bounding box represented a mere clockwise rotation of the straight edge's bounding box. This alignment ensured that during angle identification, realistic values would be displayed without the need for intentional negation.

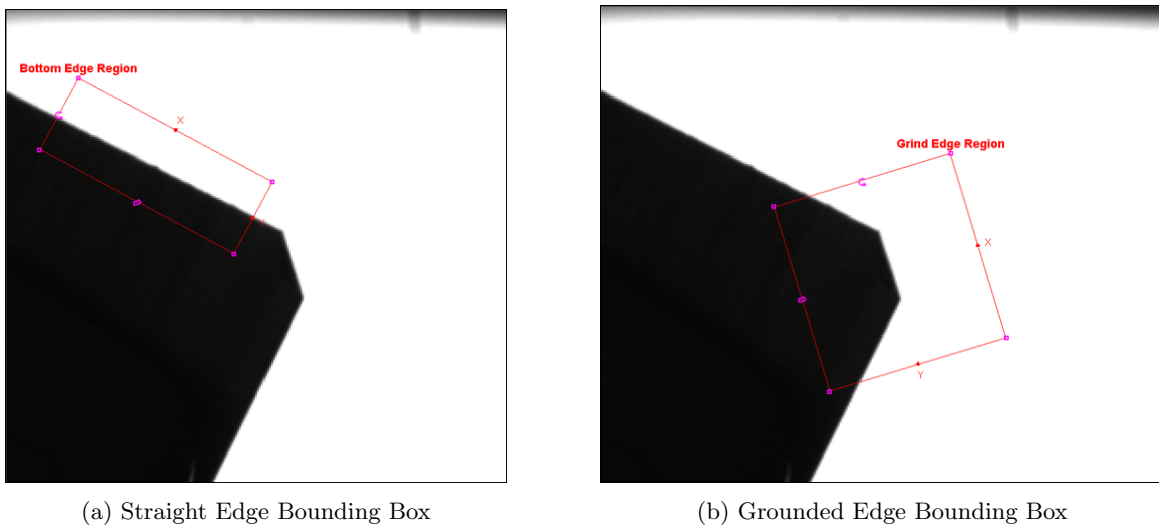


Figure 39: Edge Training

Once the pattern and edges were trained, functions within In-Sight Explorer could be leveraged to generate a detected line within the bounding boxes and utilize the GetAngle function. While a  $45^\circ$  chamfer was applied, a  $135^\circ$  angle was the detection goal. This is because as a  $45^\circ$  angle is placed on a  $90^\circ$  edge the resulting angle of the edge formulates two  $135^\circ$  angles. The entire image processing sequence can be

illustrated as shown in Figure 40. The "Row" and "Col" sections are the row and column coordinates within the image captured by camera. These coordinates denote the position of a pixel within the image matrix. For angle detection specifically, these coordinates were used to locate reference points or edges, calculate distances, to help detect the angle of the grounded edge. It's crucial to note that the system was engineered with a tolerance of  $\pm 3^\circ$ .

	A	B	C	D	E	F	G	H	I	J	K	L
0	@Image											
1												
2	Fixture											
3	Train Pattern	Region Label	Region	Train Pattern	Train							
4		Train Pattern Region	Train Pattern Region	Patterns	Train							
5	Find Pattern	Region Label	Region	Find Pattern	Index	Row	Col	Angle	Scale	Score	Pass/Fail	
6		Find Pattern Region	Find Pattern Region	Patterns	0.000	266.205	284.144	-1.512	100.015	74.507	1	
7												
8												
9	Find Edges											
10	Bottom Edge	Region Label	Region	Row	Col	High	Wide	Angle	Curve			
11		Bottom Edge Region	Bottom Edge Region	180.856	267.364	222.715	82.974	239.069	0.000			
12	Find Line	Find Line	Row0	Col0	Row1	Col1	Score	Pass/Fail				
13		Edges	215.922	246.353	101.816	55.922	-25.531	0				
14	Grind Edge	Region Label	Region	Row	Col	High	Wide	Angle	Curve			
15		Grind Edge Region	Grind Edge Region	283.997	327.798	58.156	69.732	193.787	0.000			
16	Find Line	Find Line	Row0	Col0	Row1	Col1	Score	Pass/Fail				
17		Edges	291.242	298.276	234.914	284.453	-64.017	0				
18	Grind Angle	Line to Line	Row0	Col0	Row1	Col1	Angle	Distance	Min Angle	Max Angle	Pass/Fail	Fail
19		Dist	239.413	285.557	239.413	285.557	134.719	0.000	133	137	1	0.000
20												
21												
22	Format Outputs											
23	Values	Index	Description	Value								
24		0	Find Pattern Score	74.507								
25		1	Bottom Edge Score	-25.531								
26		2	Grind Edge Score	-64.017		Tool 1	Tool 2	Tool 3				
27		3	Grind Angle	134.719		134.719	134.719	134.719				
28		4	Grind Angle Pass/Fail	1								
29	Write Outputs	Format Output Buffer	Write Results Buffer									
30		Buffer	1									
31												

Figure 40: Spreadsheet View

### 7.4.3 Data Transfer to PLC

After detecting the angle, the data needed to be transmitted to the PLC for successful transfer back to the robot. This communication was achieved using Ethernet/IP. The Format Output Buffer and Write Results Buffer functions were used to send a 32-bit integer to the PLC. To avoid any potential issues with the decimal sign, the angle value was multiplied by 1000 before transmission. Upon retrieval by the robot, the value was divided by 1000 to restore its original scale. Furthermore, the A0 cell responsible for image acquisition was switched to External mode. This configuration allowed the PLC to trigger image acquisition upon request from the RAPID program, ensuring synchronization with the robot's operation.

## 8 Data and Results

### 8.1 Mechanical Verification

Given the consistent placement of the tool by the robot, angle detection consistently fell well within the specified tolerance of  $\pm 3^\circ$ . However, to ensure reliability, angle detection wasn't solely reliant on computer vision software. To confirm the detection of a  $135^\circ$  angle, physical tools such as protractors and a 3D printed datum tool with a  $135^\circ$  angle were utilized (see Figure 41). These physical tools served as supplementary checks to validate the accuracy of the angle detection process.

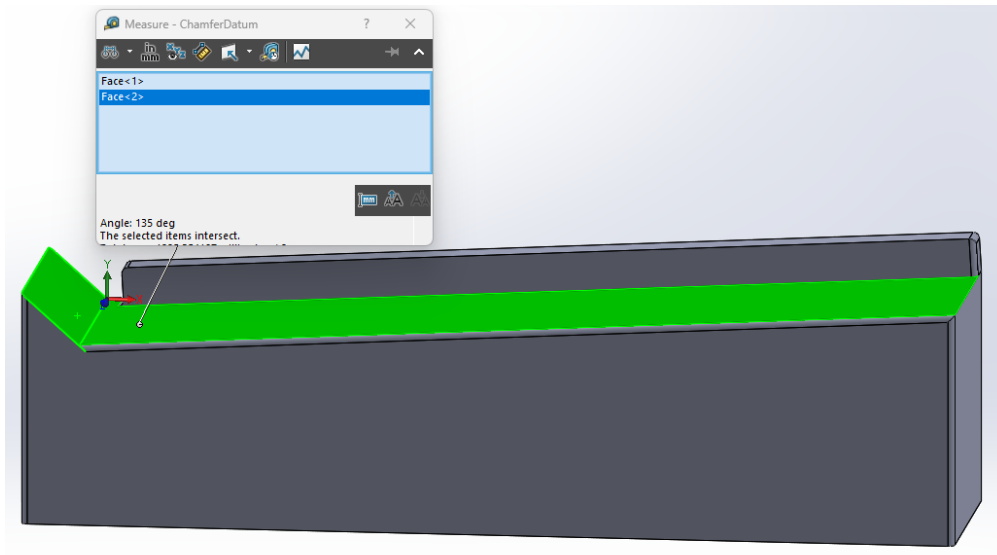


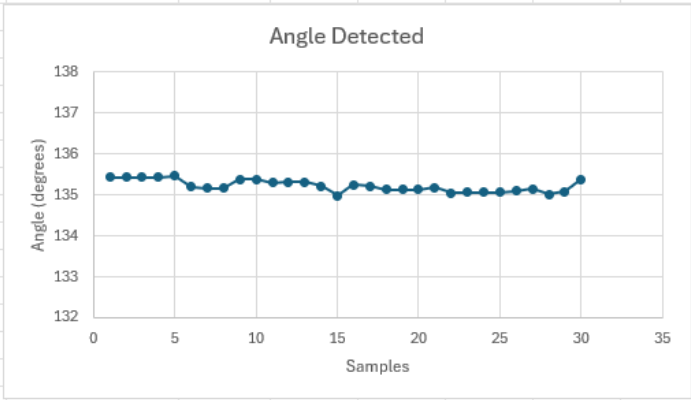
Figure 41: Mechanical Datum

### 8.2 Statistical Verification

Once iterations were conducted to ensure that the grind consistently produced a reliable  $135^\circ$  angle, samples were collected to gather statistical data and results. While over 60 samples were tested, Figure 42 includes data from 30 samples to showcase the broad range of data obtained. This involved running 30 samples consecutively and analyzing not only the average angle but also the standard deviation and percent error from the provided samples. It's important to note that this data excludes any angles detected during system calibration, focusing instead on angles obtained once the system consistently yielded data within the targeted tolerance range.

As demonstrated by the statistical data, the system proved fully capable of producing results well within the specified tolerance. In fact, the confidence level in meeting this tolerance was sufficiently high that the tolerance could potentially have been tightened to  $\pm 1^\circ$  with assurance of accuracy.

Trial Runs	Angle Detected
1	135.424
2	135.424
3	135.424
4	135.424
5	135.469
6	135.197
7	135.157
8	135.157
9	135.389
10	135.389
11	135.295
12	135.312
13	135.312
14	135.215
15	134.989
16	135.251
17	135.221
18	135.126
19	135.126
20	135.126
21	135.181
22	135.055
23	135.067
24	135.067
25	135.067
26	135.105
27	135.145
28	135.016
29	135.077
30	135.381



Mean	135.22
Standard Deviation	0.14
Percent Error	0.16%

Figure 42: Statistical Data

## 9 Discussion

### 9.1 Grind Performance

All in all, the grinds successfully achieved the criteria of displaying a  $45^\circ$  chamfer, resulting in a  $135^\circ$  angle detection. As depicted in Figure 43, the grinds appear symmetrical to the naked eye and exhibit repeatable quality. What was once considered a mundane task achievable by humans has been effectively automated, showcasing the capability of automated processes to deliver consistent results.

The outcomes of this study offer valuable insights into the potential for deployment on a larger scale. By leveraging the fundamentals of machine vision, robot integration, and force control technology, tasks of this nature are undoubtedly feasible and hold promise for various industrial applications. Furthermore, with the compact integration of the workcell, the MMET department now possesses a fully functioning workcell with integrated force control and a PLC panel. This setup can be advantageous to future professors and researchers seeking to utilize the equipment and technology within the MMET department and the college as a whole.



Figure 43: Grounded Tools

## 10 Conclusion

### 10.1 Future Improvements

While the workcell successfully achieved the desired angle grind, fulfilling the project's objectives, there remain areas ripe for improvement and further exploration. Here are some key points:

- The workcell lacks an external E-stop, separate from the one on the robotic Teach Pendant. While the Teach Pendant's E-stop halts the robot's movement, it doesn't de-energize the entire cell, including external devices like the belt sander, backlight, and Cognex camera. Incorporating an additional E-stop enhances the overall safety of the workcell.
- Electrical schematics for the PLC panel are absent. While the wiring layout follows color coordination, documented schematics are essential for clear understanding of power flow throughout the workcell.
- The workcell currently lacks an automated cleaning system. After a grind cycle, debris removal relies on manual use of a handheld vacuum. Researching and implementing an automated vacuuming system would enhance safety by preventing grind debris from spreading within the cell.
- Consideration should be given to incorporating an HMI stand. HMIs (Human Machine Interfaces) are prevalent in industry for remote operation of workcells. Developing an HMI stand, either by purchasing an external table stand or mounting a slimmer panel to a podium-like stand, would align the workcell with industrial standards and improve usability.

### 10.2 Project Hurdles and Lessons Learned

Stepping away from the formal tone of earlier sections, I humbly present myself in this section sharing some personal reflections on the lessons learned and conclusions drawn from my journey through this graduate capstone project. From crafting the problem statement in June 2023 to achieving completion in May 2024, this project has been a whirlwind of experiences that have enriched my understanding of robotics, automation, and the essence of engineering problem-solving. Throughout the project's lifecycle, I've encountered numerous challenges, made mistakes, and adapted plans accordingly. Below are a few examples:

- Entering this project, I lacked crucial knowledge in PLC programming and panel design, especially in creating electrical schematics. This gap delayed progress as I relied on online research, assistance from professors, and intuition when it came to designing and wiring the PLC panel, as well as programming the logic for the PLC. Moving forward, I'll prioritize filling knowledge gaps before starting projects.
- The expected footprint of this workcell changed from 36" x 28". This resulted in me having to re-engineer the layout for the cell as well as the overall robotic pathing for the entire manufacturing process.
- During the force control aspect of the project, I observed that the gripper and the aluminum tool lacked sufficient friction to withstand the applied torque on the tool edge. Although I devised solutions by adjusting pickup placement and modifying robotic pathing, I realized that developing a gripper with rubber feet or a locking mechanism for the tool could have provided a more robust and secure integration.
- While the mechanical datum and protractor visually assured that the chamfer was indeed 45° across the entire tool's thickness, I noticed a limitation in the vision system's inspection. It only examined



one side of the tool. If I were to approach this project again, I would implement a procedure for the robot to flip the tool over, allowing for inspection of both sides. This would ensure confirmation of a consistent 45° chamfer across the entire edge.

## References

- [1] ABB. *Application manual - EtherNet/IP Scanner/Adapter*. URL: <https://library.e.abb.com/public/4e0ac7869dcc435cbe2e2fb32b9b7d22/3HAC050998%20AM%20EtherNetIP%20Scanner%20Adapter%20RW%206-en.pdf?x-sign=Tvd/qFrAgEdcEN0tz1S1jtjiJgCXDOIPwMdHyZASfNh0/+fpaIrDX5WzkybjH93P>.
- [2] ABB. *Application manual - Scalable I/O*. URL: <https://library.e.abb.com/public/6ad013fab36843cdb0eab366d0ac3HAC059109%20AM%20Scalable%20IO%20RW%206-en.pdf?x-sign=V4Brpgliv7mryUBKp3CPN06A9G5bz318zAudwNjcd3uJ>.
- [3] Gary Mitchell Bone et al. "Force Control for Robotic Deburring". In: *Journal of Dynamic Systems, Measurement, and Control* 113.3 (1991), pp. 395–400.
- [4] Brady Corporation. *Wiring Color Codes - NEC Electrical Standards 3-Phase*. URL: <https://www.bradyid.com/resources/wiring-color-codes>.
- [5] Cognex Corporation. *In-Sight Explorer: Communications to/from Rockwell 1756-L72S*. URL: <https://support.cognex.com/en/downloads/detail/in-sight/2722/1033>.
- [6] A. Pillai et al. *Burr Registration Using Image Processing*. Advances in Industrial Machines and Mechanisms. tech. Nagpur, India: Springer, 2021.

# 11 Appendix A

(Ladder Logic on following page)

PLC Control Program

